

Research Advances

Zircon SIMS U-Pb Age of the Shaxinan Melagabbro, Eastern Tianshan and Constraints on Fe-Ti-V Oxide Mineralization

SHI Yu^{1,2,*}, WANG Yuwang¹, WANG Jingbin^{1,2}, MAO Qigui¹, XIE Hongjing¹, ZHOU Guochao², ZHU Jiangjian¹, WEI Xiaofeng¹ and LÜ Xiaoqiang¹

¹ Beijing Institute of Geology for Mineral Resources, Beijing 100012, China

² School of Earth Sciences and Resources, China University of Geosciences, Beijing 100083, China

Objective

The late Paleozoic Fe-Ti-V oxide deposit of the eastern Tianshan is an important orthomagmatic deposit type in the Central Asia Orogenic Belt (CAOB). A series of Fe-Ti-V oxide deposits and mineralized mafic-ultramafic intrusions have been recognized recently, such as those in Hongliangzi, Weiya, Yaxi, Shaxinan and Shaxi on the Central Tianshan massif, and Niumaoquan on the southern margin of the Harlik belt (Shi et al., 2018a). Only a few Fe-Ti-V oxide deposits in the eastern Tianshan (e.g., Weiya and Niumaoquan) have been studied, and their chronology need to be further constrained for study of regional Fe-Ti-V oxide metallogenic mechanism and variation of mantle-derived magmas during the orogenic process.

The Shaxinan deposit is hosted in a layered gabbroic intrusion occurring on the northern margin of the Central Tianshan massif, and is one of the typical Fe-Ti-V oxide deposits in the eastern Tianshan. A zircon SIMS U-Pb geochronological study has been carried out for the first time in this paper, in order to obtain a precise and accurate crystallization age for the Shaxinan layered gabbroic intrusion, and to further evaluate its Fe-Ti-V oxide mineralization age.

Methods

Zircon grains from melagabbro of the Shaxinan Fe-Ti-V oxide deposit at 41°42'28.38"N and 92°42'11.10"E were separated using conventional magnetic and density techniques. These grains, together with the zircon standards TEMORA and Qinghu, were mounted in epoxy resin. The mounts were polished to expose the centers of the grains. U-Pb isotopes of zircon crystals were determined at the analytical laboratory of Beijing Research Institute of Uranium Geology. Measurements of U, Th and Pb were conducted by using the CAMECA IMS 1280 ion microprobe. The measured Pb isotopic

compositions were corrected for common Pb by using non-radiogenic ²⁰⁴Pb. The corrections were satisfactorily small to be insensitive to the preference for common Pb composition. An average of the present-day crustal composition was used for the common Pb. The uncertainties of individual analyses were reported at a 1 sigma level; the mean ages for pooled U-Pb analyses were quoted with a 95% confidence interval.

Results

Zircons from the sample vary from euhedral to anhedral with most occurring as crystal fragments with rounded terminations from initially equant to short or long prismatic crystals (Fig. 1a). Most crystals display oscillatory or patchy linear zoning with variable luminescence in CL images (Fig. 1a). U and Th contents vary from 226 to 1119 ppm and 95 to 1155 ppm, respectively (Appendix 1). All zircon grains exhibited concentric zoning, their well-developed crystal shape, internal banding, and high Th/U ratios (0.38–1.05) were consistent with a mafic igneous origin (Fig. 1a; Appendix 1). The analyses are clustered on a U-Pb Concordia curve (Fig. 1b), yielding a concordia age of 307.3 ± 4.4 Ma (Fig. 1b, MSWD = 0.41), which is interpreted as the Shaxinan gabbroic intrusion's crystallization age.

Conclusions

The zircon grains from the Shaxinan melagabbro hosting a Fe-Ti-V oxide deposit analyzed in this study yielded a concordia age of 307.3 ± 4.4 Ma (Fig. 1b), which is similar to the Niumaoquan Fe-Ti-V oxide deposit formed in the Late Carboniferous (Shi et al., 2018a), and slightly older than the mafic-ultramafic intrusions hosting Ni-Cu sulfide deposits and CuNi-VTiFe composite deposit in the eastern Tianshan (Qin et al., 2011; Shi et al., 2018b), suggesting that the Fe-Ti-V oxide mineralization possibly formed by different mantle derived magmatism

* Corresponding author. E-mail: orounaxiong@sina.com

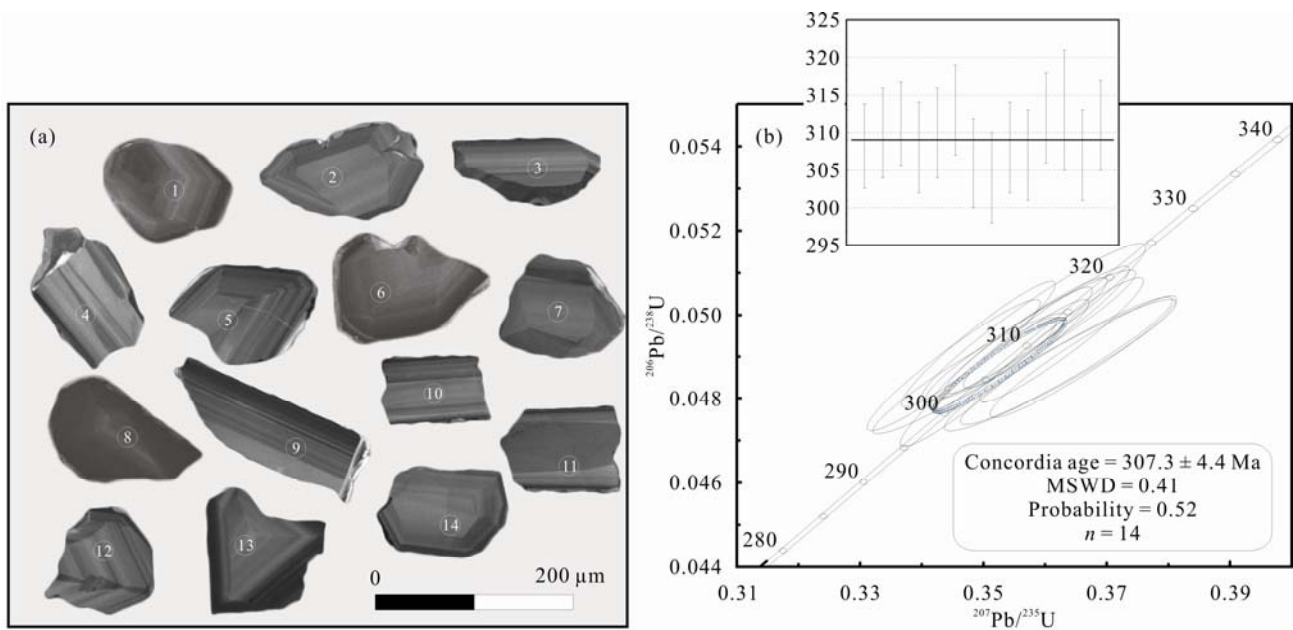


Fig. 1. (a) Cathodoluminescence images and (b) zircon U-Pb Concordia plot for the Shaxinan melagabbro.

during the orogenic process.

Acknowledgments

This study is financially supported by the National Key R&D Program of China (Grant No. 2017YFC0601204).

References

Qin, K.Z., Sun, B.X., Sakyi, P.A., Tang, D.M., Li, X.H., Sun, H., Xiao, Q.H., and Liu, P.P., 2011. SIMS zircon U-Pb geochronology and Sr-Nd isotopes of Ni-Cu-bearing mafic-ultramafic intrusions in eastern Tianshan and Beishan in correlation with flood basalts in Tarim basin (NW China):

constraints on a ca. 280 Ma mantle plume. *American J. Sci.*, 311: 237–260.

Shi Yu, Wang Yuwang, Wang Jingbin, Xie Hongjing, Mao Qigui, Zhao Lutong, Long Lingli, Li Dedong and Zhou Guochao, 2018a. Petrogenesis and metallogenesis of the Niunaoquan gabbroic intrusion associated with Fe-Ti oxide ores in eastern Tianshan, NW China. *Acta Geologica Sinica* (English Edition) (in press).

Shi Yu, Wang Yuwang, Wang Jingbin, Zhao Lutong, Xie Hongjing, Long Lingli, Zou Tao, Li Dedong and Zhou Guochao, 2018b. Physicochemical control of the Early Permian Xiangshan Fe-Ti oxide deposit in eastern Tianshan (Xinjiang), NW China. *J. Earth Sci.*, 29(3): 520–526.

Appendix 1 SIMS zircon U-Pb dating results of the Shaxinan melagabbro

Sample	Content (ppm)		Th/U	Isotopic ratios				Apparent age (Ma)							
	U	Th		$^{207}\text{Pb}/^{235}\text{U}$	1 σ	$^{206}\text{Pb}/^{238}\text{U}$	1 σ	$^{207}\text{Pb}/^{206}\text{Pb}$	1 σ	$^{207}\text{Pb}/^{235}\text{U}$	1 σ	$^{206}\text{Pb}/^{238}\text{U}$	1 σ	$^{207}\text{Pb}/^{206}\text{Pb}$	1 σ
Sxn@01	804	678	0.84	0.35476	0.00819	0.0490	0.0009	0.0525	0.0007	308.3	6.2	308.2	5.6	308.6	31.3
Sxn@02	688	551	0.80	0.35440	0.00879	0.0492	0.0010	0.0522	0.0008	308.0	7.0	310.0	6.0	294.0	34.0
Sxn@03	587	358	0.61	0.35692	0.00871	0.0495	0.0009	0.0523	0.0008	309.9	6.5	311.2	5.6	300.5	35.7
Sxn@04	493	341	0.69	0.36620	0.01000	0.0490	0.0010	0.0542	0.0010	317.0	7.0	308.0	6.0	379.0	42.0
Sxn@05	1037	569	0.55	0.34920	0.00824	0.0493	0.0010	0.0514	0.0006	304.0	6.0	310.0	6.0	257.0	28.0
Sxn@06	550	424	0.77	0.36020	0.00890	0.0497	0.0010	0.0526	0.0008	312.0	7.0	313.0	6.0	310.0	35.0
Sxn@07	506	277	0.55	0.34781	0.01036	0.0486	0.0010	0.0519	0.0012	303.1	7.8	305.9	5.9	281.5	50.6
Sxn@08	920	970	1.05	0.34920	0.00838	0.0484	0.0010	0.0524	0.0006	304.0	6.0	304.0	6.0	302.0	26.0
Sxn@09	352	134	0.38	0.36350	0.01138	0.0489	0.0010	0.0539	0.0013	315.0	9.0	308.0	6.0	365.0	52.0
Sxn@10	504	335	0.66	0.34520	0.00929	0.0488	0.0010	0.0513	0.0009	301.0	7.0	307.0	6.0	253.0	38.0
Sxn@11	226	950	0.42	0.35770	0.01123	0.0495	0.0010	0.0524	0.0012	310.0	8.0	312.0	6.0	302.0	53.0
Sxn@12	236	163	0.69	0.35810	0.01203	0.0498	0.0012	0.0521	0.0012	311.0	9.0	313.0	8.0	292.0	50.0
Sxn@13	259	102	0.39	0.36250	0.01243	0.0488	0.0010	0.0539	0.0014	314.0	9.0	307.0	6.0	368.0	59.0
Sxn@14	1119	1155	1.03	0.36270	0.00878	0.0494	0.0010	0.0533	0.0007	314.0	7.0	311.0	6.0	340.0	31.0